

The Far-Infrared Properties of Spatially Resolved AKARI Observations*

Woong-Seob JEONG,¹ Takao NAKAGAWA,¹ Issei YAMAMURA,¹ Chris P. PEARSON,^{1,2}
Richard S. SAVAGE,³ Hyung Mok LEE,⁴ Hiroshi SHIBAI,⁵ Sin'itirou MAKIUTI,¹ Hajime BABA,⁶
Peter BARTHEL,⁷ Dave CLEMENTS,⁸ Yasuo DOI,¹ Elysandra FIGUEREDO,⁹ Tomotsugu GOTO,¹
Sunao HASEGAWA,¹ Hidehiro KANEDA,¹ Mitsunobu KAWADA,⁵ Akiko KAWAMURA,⁵ Do KESTER,¹⁰
Suk Minn KWON,¹¹ Hideo MATSUHARA,¹ Shuji MATSUURA,¹ Hiroshi MURAKAMI,¹ Sang Hoon OH,⁴
Sebastian OLIVER,³ Soojong PAK,¹² Yong-Sun PARK,⁴ Stephen SERJEANT,⁹
Mai SHIRAHATA,¹ Jungjoo SOHN,⁴ Toshinobu TAKAGI,¹ Lingyu WANG,⁸ Glenn J. WHITE,^{9,13}
and Chisato YAMAUCHI¹

¹*Institute of Space and Astronautical Science, Japan Aerospace Exploration Agency,
Yoshinodai 3-1-1, Sagami-hara, Kanagawa 229-8510*

jeongws@ir.isas.jaxa.jp

²*European Space Astronomy Centre (ESAC), Apartado 50727, 28080 Madrid, Spain*

³*Astronomy Centre, Department of Physics and Astronomy, University of Sussex, Brighton BN1 9QH, UK*

⁴*Department of Physics and Astronomy, Seoul National University, Shillim-dong, Kwanak-gu, Seoul 151-742, South Korea*

⁵*Infrared Astrophysics Laboratory, Nagoya University, Furo-cho, Chikusa-ku, Nagoya 464-8602*

⁶*Center for Research and Development, University of Education, Ibaraki University, 2-1-1 Bunkyo, Mito, Ibaraki 310-8512*

⁷*Kapteyn Astronomical Institute, University of Groningen, P.O. Box 800, 9700 AV Groningen, The Netherlands*

⁸*Astrophysics Group, Imperial College London, Blackett Laboratory, Prince Consort Road, London SW7 2AZ, UK*

⁹*Department of Physics and Astronomy, The Open University, Walton Hall, Milton Keynes MK7 6AA, UK*

¹⁰*Netherlands Institute for Space Research SRON, Postbus 800, 9700 AV Groningen, The Netherlands*

¹¹*Department of Science Education, Kangwon National University, Hyoja-dong, Chunchon-si, Kangwon-do 200-701, South Korea*

¹²*Department of Astronomy and Space Science, Kyung Hee University,*

1 Seocheon-dong, Giheung-gu, Yongin-si, Gyeonggi-do 446-701, South Korea

¹³*Space Science & Technology Department, CCLRC Rutherford, Appleton Laboratory, Chilton, Didcot, Oxfordshire OX11 0QX, UK*

(Received 2007 March 3; accepted 2007 July 31)

Abstract

We present spatially resolved observations of IRAS sources from the Japanese infrared astronomy satellite AKARI All-Sky Survey during the performance verification phase of the mission. We extracted reliable point sources matched with the IRAS point source catalogue. By comparing IRAS and AKARI fluxes, we found that the flux measurements of some IRAS sources could have been over or underestimated, and affected by the local background, rather than the global background. We also found possible candidates for new AKARI sources and confirmed that AKARI observations resolved IRAS sources into multiple sources. All-Sky Survey observations are expected to verify the accuracies of IRAS flux measurements and to find new extragalactic point sources.

Key words: galaxies: photometry — infrared: galaxies — ISM: structure — space vehicles

1. Introduction

The Infrared Astronomy Satellite mission (IRAS) (Soifer et al. 1987) successfully performed the first all-sky survey at infrared wavelengths, providing many fruitful results. After this pioneering mission over two decades ago, the AKARI satellite (previously known as ASTRO-F) (Murakami 1998; Nakagawa 2001; Shibai 2004; Pearson et al. 2004; Murakami et al. 2007) is performing the next-generation all-sky survey, primarily with the FIS (Far-Infrared Surveyor) focal plane instrument in 4 far-IR bands (50–200 μm range) to improved the spatial resolutions and wider wavelength coverage than the its predecessor IRAS [see Kawada et al. (2007) for detailed specifications and hardware performance

of the FIS instrument].

Although the telescope apertures of IRAS (60 cm) and AKARI (68.5 cm) are similar, the effective beam size of the AKARI mission (0.5–0.9) is much smaller than that of IRAS (2'–5') because the sizes of the detector pixels in IRAS were much larger than the size of the diffracted beam of the telescope. Due to this relatively large beam size, the astronomical observations made in the far-IR bands of the IRAS mission were presumed to have been affected by the fluctuation noise arising from both the background structures and many overlapping extragalactic point sources below the resolution of the beam. As the resolution of the telescope/instrument beam increases, the measurements of point source fluxes are less prone to fluctuation noises. Thus, fluctuation noise needs to be more carefully treated for the accurate extraction of sources and flux measurements [see Jeong et al. (2005, 2006) for realistic estimations of these

* Based on observations with AKARI, a JAXA project with the participation of ESA.

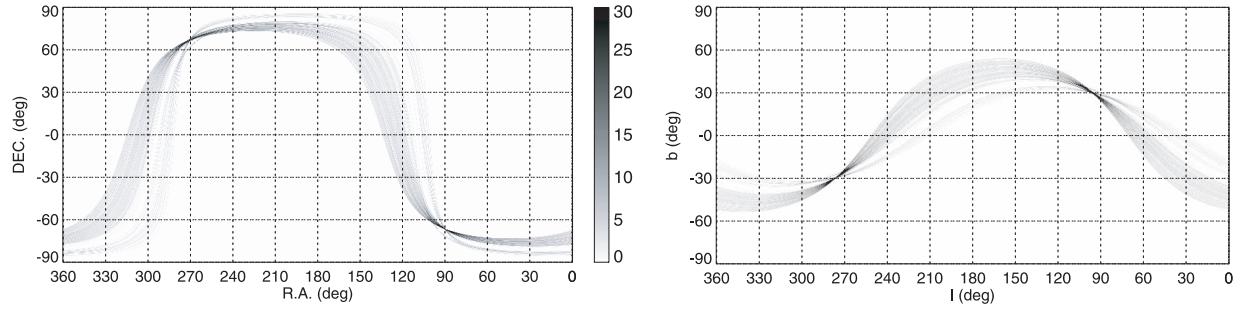


Fig. 1. Scan map area during the Performance Verification (PV) phase in equatorial coordinates (left) and galactic coordinates (right). The gray bar shows the number of orbit surveyed by AKARI. Due to the nature of AKARI orbit, the regions near the North Ecliptic Pole (NEP) and the South Ecliptic Pole (SEP) have visibility significantly higher than other regions on the celestial sphere.

noises for the AKARI mission]. From observations of sources for those with IRAS fluxes made during the Performance Verification (PV) phase of the AKARI, we have investigated how the resolved background near a point source can affect the measurement of fluxes by comparing the measured fluxes.

This paper is organized as follows. In section 2, we describe the data and the data reduction. We present a comparison of our results between the IRAS flux and the AKARI flux in section 3. The probable detections of new AKARI sources are explained in section 4. We summarize our results in section 5.

2. AKARI All-Sky Observation and Data Reduction

The data used in this work are from AKARI All-Sky Survey observations performed during the two week-long PV phase from 2006 April 24 to May 7. The observations cover a range in galactic latitude between -50° to 50° , as shown in figure 1.

For data processing, we have used the latest pipeline developed for the All-Sky Survey (A. Kawamura et al. 2003 informed by the Internal ISAS report). Source extraction was performed only for the AKARI *WIDE-S* band ($90\ \mu\text{m}$) with the dedicated software for the AKARI survey. Concerning the purpose of calibrating the absolute flux, the observations of asteroids, stars, and galaxies with a wide range of fluxes were used, and the uncertainty of flux calibration is expected to be less than 20% for the *WIDE-S* band (Kawada et al. 2007). In order to avoid false detections, we removed any detections near the South Atlantic Anomaly (SAA) region, reset or calibration sequences and the edge of a detector array. Among the extracted sources, we have selected reliable sources with the following criteria to eliminate false detections: (1) signal-to-noise ratio (S/N) greater than 15, (2) detected in all rows of the detector array, e.g., 3 rows of detector pixels for the *WIDE-S* band, and (3) confirmed in at least two more orbits (~ 100 m per 1 orbit for AKARI) (4) the galactic plane region is excluded, because it is observed in a special detector readout mode that needs separate processing [for the sampling mode of AKARI observation, see Kawada et al. (2007) for detailed information]. After selecting reliable sources, we attempted to match them with IRAS sources within a positional error circle of $100''$. The total number of sources in our final selected sample is 150. We show the positional difference between the AKARI and IRAS sources with a good flux quality in figure 2. Most of the positions for IRAS sources

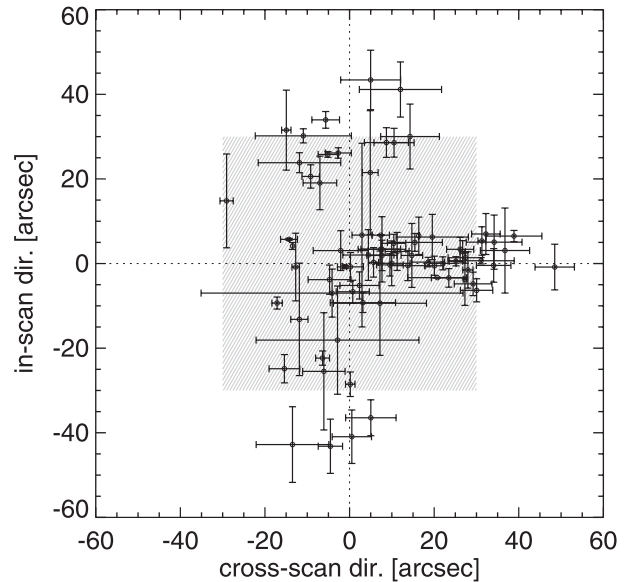


Fig. 2. Positional difference between IRAS and AKARI for samples with a good IRAS flux quality. The shaded area means the pixel size of AKARI/FIS for the *WIDE-S* band ($30''$). Since we only plot sources confirmed in at least two more orbits, the error bar means the standard deviation of positions in in-scan and cross-scan directions.

are very consistent with those estimated in AKARI within the resolution range ($30''$). The current position information was determined based on the sensors of the onboard attitude and orbit control system (AOCS), reprocessed on the ground. The major source of uncertainty is the alignment between the AOCS sensors and the telescope, and its time variation. In the future, position information will be improved by pointing reconstruction processing using the data from the focal-plane instruments. The accuracy of the detected source position will be as good as a few arcseconds, which will enable us to carry out more detailed analyses of the ‘IRAS’ positions. Figure 3 shows the distribution of these sources in ecliptic coordinates.

3. A Comparative Study of AKARI and IRAS Fluxes

The reliably detected sources are used to compare the IRAS and AKARI fluxes.

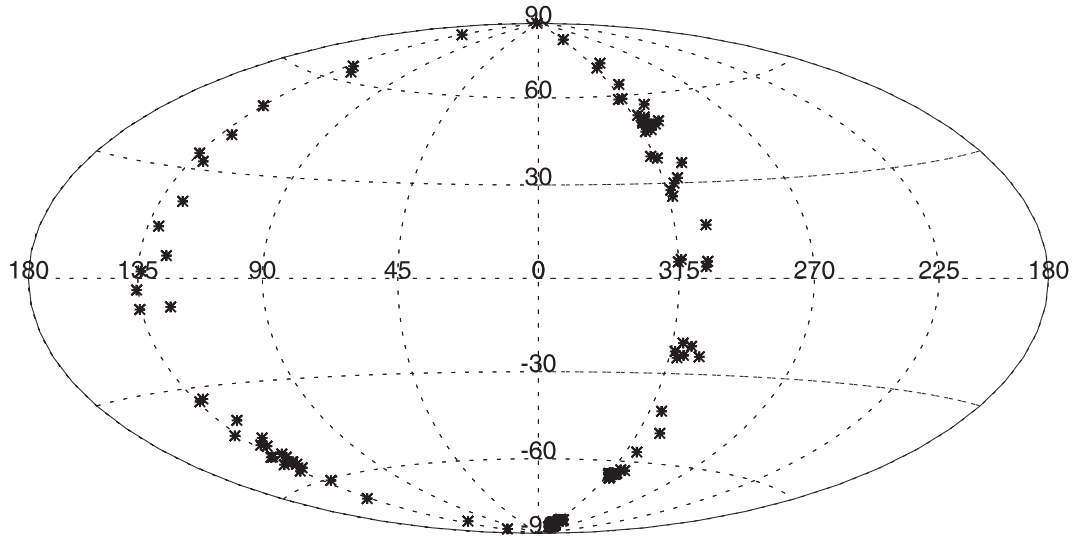


Fig. 3. Distribution of sources matched with the IRAS catalogue in ecliptic coordinates.

3.1. Flux Comparison

The effective wavelength of the AKARI *WIDE-S* band is $90\ \mu\text{m}$, while IRAS has $60\ \mu\text{m}$ and $100\ \mu\text{m}$ bands in the far-IR region. In order to make a consistent comparison between the AKARI and IRAS fluxes, we computed the IRAS flux at $90\ \mu\text{m}$ by fitting the $60\ \mu\text{m}$ and $100\ \mu\text{m}$ data to a black-body curve. Since the flux densities of the IRAS point sources listed in the catalogue are non-color corrected ones, we attempted an iterative fitting method, which performs successively fitting and color corrections. We also applied color correction to the AKARI flux densities. Figure 4 shows the comparison between the AKARI and IRAS fluxes of our detected sources at $90\ \mu\text{m}$. We also plot the error bars for the IRAS and AKARI fluxes. Note that the flux error for an AKARI flux was obtained from the standard deviation of the extracted fluxes for orbit-confirmed detections, while the flux error for the IRAS sources with a bad flux quality was not listed in the IRAS point-source catalogue. The straight line shows a perfect correlation between these two fluxes. The size of the circle is proportional to the estimated signal-to-noise ratio. This figure shows that the data lies below the envelope of $F_{\text{AKARI}} \approx F_{\text{IRAS}}$. This means that the AKARI fluxes are in general similar to, or smaller than, the IRAS fluxes.

Such a trend is more clearly shown in figure 5, which displays the flux ratio of IRAS to AKARI detections. We checked the quality of the IRAS flux, by examining the quality flag for the deviating sources. Most of those sources indeed have a moderate or a bad flux quality, and are often located near the galactic plane or strong star-formation regions (e.g., Large Magellanic Cloud). Thus, due to a strong background, the flux of IRAS sources with moderate or bad flux quality flags may not have been accurately estimated. We also found that the flux is over or underestimated even for IRAS sources with a high flux quality. The scattering trend in flux ratio shows a triangular shape (peaking at $80\ \text{Jy}$) in the upper panel of figure 5 and a right triangular shape in the lower panel of figure 5, respectively. The sensitivity of AKARI in the low-flux

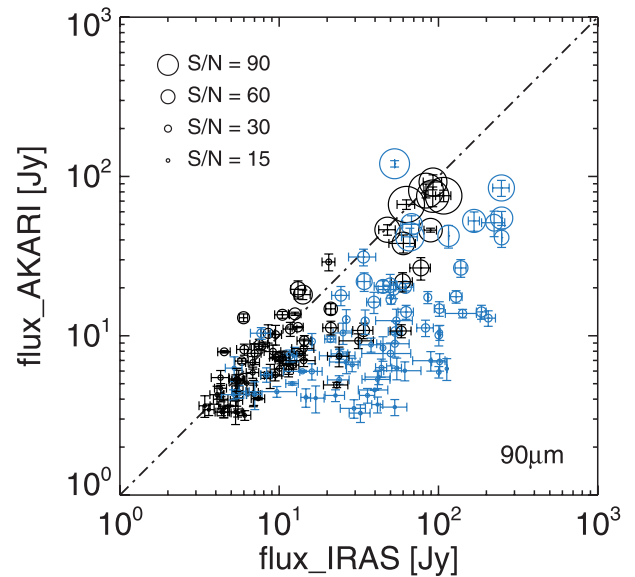


Fig. 4. Comparison of the flux between IRAS and AKARI. The larger symbol means detection with a larger S/N. The black symbols are for IRAS sources with a high flux quality both in $60\ \mu\text{m}$ and $100\ \mu\text{m}$; the other cases are displayed in half-tone symbols. We also plot the error bars for the AKARI and IRAS flux.

range is better than that of IRAS, which explains that the scatter in the lower panel of figure 5 is larger for low fluxes than for high fluxes.

3.2. Effect of the Background on the Flux Estimation

The background fluctuations from the surface brightness of an extended structure can easily be mistaken for genuine point sources. Since our detections are for bright sources, the contribution of the fluctuation noise will be primarily from sky confusion (rather than point sources). Some authors have estimated sky confusion from background fluctuations for the AKARI mission based upon IRAS and ISO data (Jeong et al.

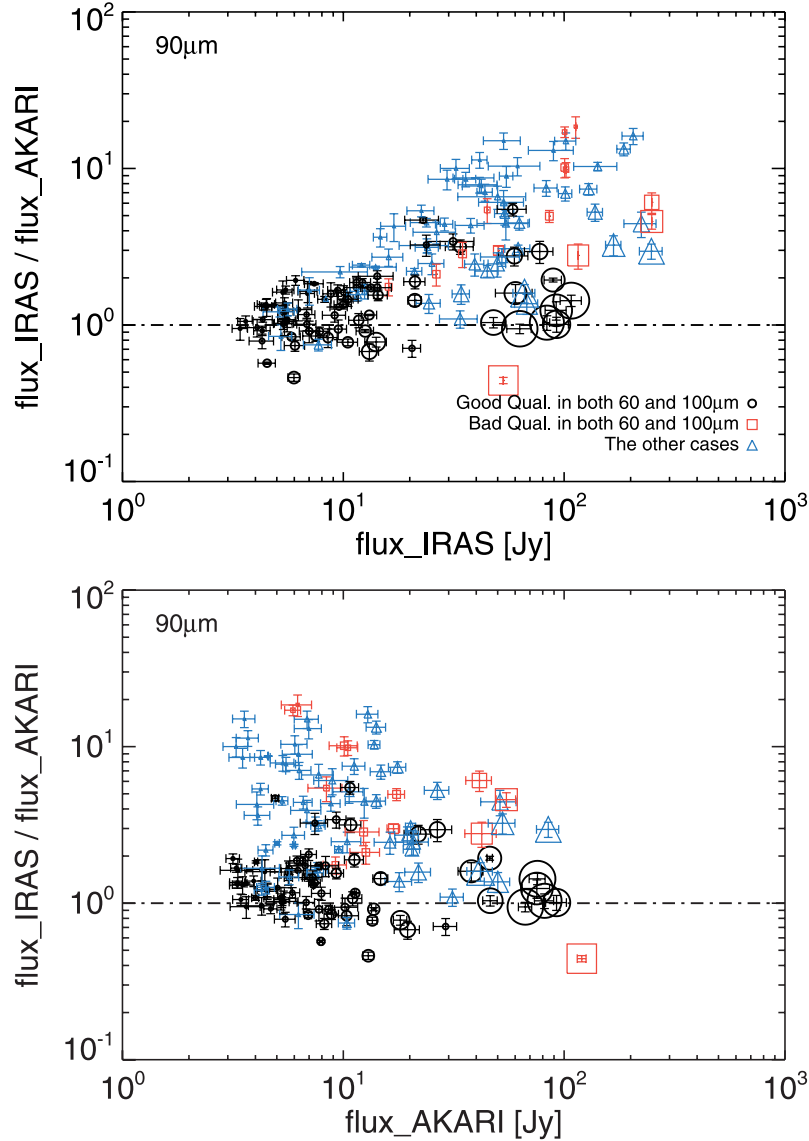


Fig. 5. Flux ratios of IRAS to AKARI flux measurements as a function of the IRAS flux (upper) and the AKARI flux (lower).

2005; Kiss et al. 2005). In order to check for any dependence of the flux uncertainty on the background level, we plot flux ratios as a function of the background emission in figure 6. We assume that the fluctuations from the background are mainly from cirrus emission. The fluctuations from zodiacal light is expected to be small at the resolution of the IRAS mission. For estimating of the cirrus emission in the AKARI band, we used an all-sky $100\mu\text{m}$ dust map generated from the IRAS and COBE data by Schlegel, Finkbeiner, and Davis (1998) and a dust model by Finkbeiner et al. (1999). As shown in the upper panel of figure 6, the scatter increases around the 20 MJy sr^{-1} level, with an underlying monotonic increase from 20 to 200 MJy sr^{-1} . Owing to its higher resolution, AKARI can resolve the background more effectively. Since the estimated background for IRAS depends on the relatively larger spatial structure of the background compared to the diffracted beam size [the source extraction for IRAS used an annulus of radius $5' - 7'$ in measuring the background

(Wheelock et al. 1994)], it could not be measured properly on a intensively fluctuating background. Therefore, this trend shows that the local background at least below $5'$ near a source, rather than the global background, is an important factor in the flux estimation. Note that previous estimations of sky confusion (Jeong et al. 2005; Kiss et al. 2005) suggested that the fluctuation noise is strongly dependent on the background level with the assumption that the spatial power spectrum from fluctuations of the dust emission has a simple power-law with a power index of ~ -3 (Gautier et al. 1992). In addition, we have also made a simple estimation of the contamination of the flux by summing the background flux over a detector pixel. We plot the case for a 10 Jy IRAS source contaminated by a 10% background (see the dotted line in figure 6). We found that flux measurements for some IRAS sources might be contaminated by the background. If we plot AKARI sources matched with IRAS sources with only high flux quality flags (see the lower panel of figure 6), the scatter is reduced,

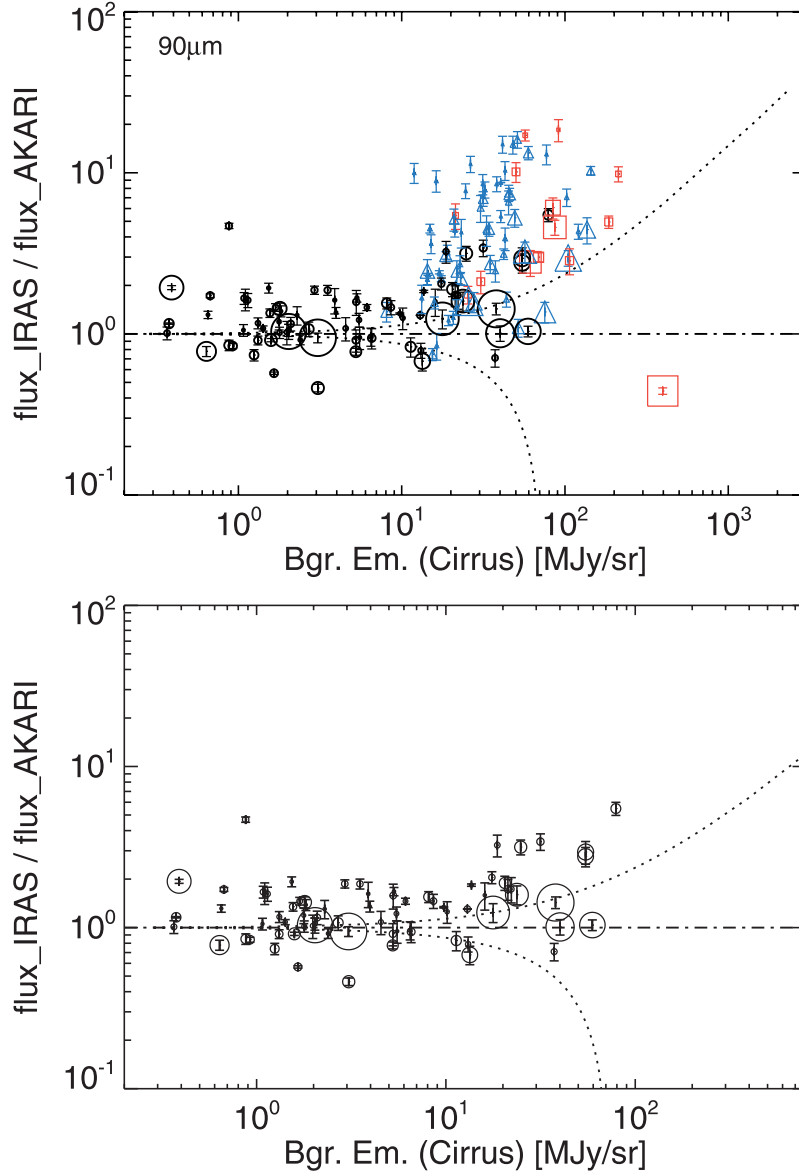


Fig. 6. Ratio of IRAS to AKARI flux measurements. We plot all matched sources (upper) and sources matched with IRAS sources with a high quality flag (lower). The dotted line shows the expected contamination from the background for 10 Jy source. The explanations for symbols are the same in the figures 4 and 5.

however, visible scatter still remains, and slightly increases as the cirrus background becomes larger. Thus, IRAS flux measurements may have errors even for correctly measured IRAS sources with a high flux quality. For a more systematic study to confirm this result, we need to use samples from a wider survey area.

4. New AKARI Sources

In this work, we used only sources matched with the IRAS point-source catalogue. However, we also detected new sources from the AKARI All-Sky Survey that are not present in the IRAS catalogue. There are many possible candidates for these new AKARI sources. First, one IRAS source may

have been resolved into two sources (see one example shown in figure 7). Second, some sources may be resolved from the background. Third, the source may be a Solar System object, e.g., asteroid. Fourth, some detections may be false due to the detector characteristics. On the other hand, there may be false detections from IRAS. Thus, we expect that the AKARI All-Sky Survey can find new extragalactic point sources as well as faint galactic point sources.

5. Summary

By using the AKARI All-Sky Survey data taken during the PV phase, we tried to extract reliably detected sources and compared their fluxes with associations in the IRAS

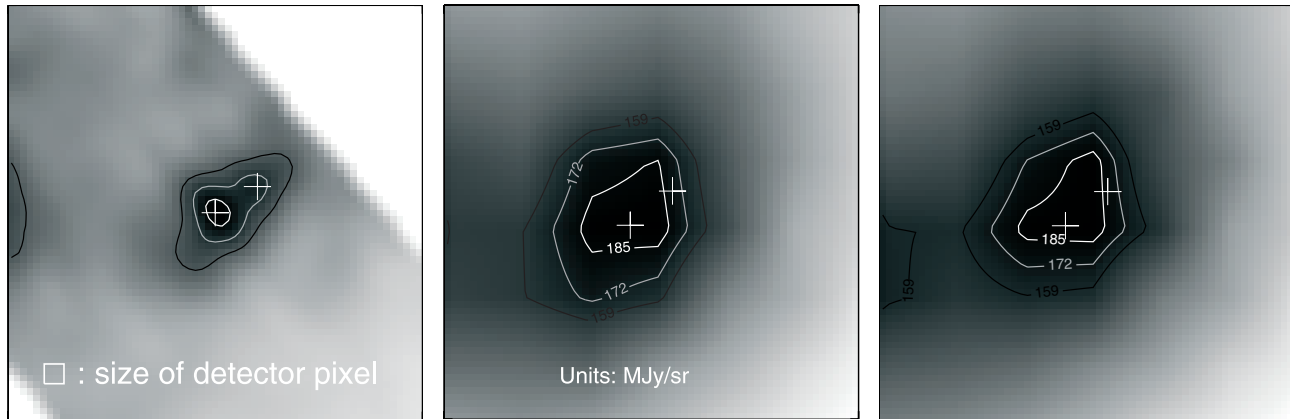


Fig. 7. Detection image for IRAS 05360–6914 with a size of $10'.5 \times 10'.5$ from AKARI $90 \mu\text{m}$ (left), IRAS $60 \mu\text{m}$ (center), and $100 \mu\text{m}$ (right) map in linear gray scale for flux. We used the revised IRAS map by Miville-Deschênes and Lagache (2005), which included well-calibrated point sources and corrected diffuse emission calibration. Since AKARI image is not calibrated yet, we did not show contour levels. The flux for the IRAS source listed in the catalogue is $61.67 (60 \mu\text{m})$ and $251.8 \text{ Jy} (100 \mu\text{m})$, and the flux quality was measured to be bad ($60 \mu\text{m}$) and moderate ($100 \mu\text{m}$). Owing to the higher resolution of AKARI, this IRAS source was detected as two sources in the AKARI observation. In addition, we found that the flux estimated from IRAS is also overestimated in this detection by a factor of ~ 5 . The plus symbols mean the positions of two detected sources.

point-source catalogue. The positions of IRAS sources are mostly very consistent with those estimated from AKARI. We found that the original flux measurements of some IRAS sources appear to have been overestimated or underestimated. We also confirmed that most of the IRAS sources with a moderate or a bad quality flux flag in the IRAS catalogue were quite overestimated. To investigate any possible contamination of the IRAS source flux from the background in the estimation of the flux, we checked the background level on each detection of the IRAS sources. The difference in the flux between the IRAS and AKARI associations was not found to be strongly dependent on the background level. However, it is suggested that the flux measurement may have been affected by the local background, rather than the global background. Note that AKARI can resolve the background and source more effectively than IRAS, due to the higher resolution of the AKARI observations. In addition, we found that in some cases, the flux measurements even for correctly measured (high flux quality) IRAS sources may include errors of up to ~ 5 , even though we consider the uncertainty of the flux calibration. However, due to various detector characteristics, there may be false detections as well as detections with inaccurately estimated flux, though we removed false detections and selected reliable detections, as described in section 2. The AKARI All-Sky Survey is expected

both to verify the IRAS sources and to find new extragalactic or galactic point sources. A preliminary catalogue for reliably detected point sources will be released in a forthcoming paper.

The AKARI Project is an infrared mission of the Japan Space Exploration Agency (JAXA) Institute of Space and Astronautical Science (ISAS), and is carried out with the participation of mainly the following institutes; Nagoya University, The University of Tokyo, National Astronomical Observatory of Japan, The European Space Agency (ESA), Imperial College London, University of Sussex, The Open University (UK), University of Groningen / SRON (The Netherlands), Seoul National University (Korea). The far-infrared detectors were developed under collaboration with The National Institute of Information and Communications Technology. We would like to thank the referee L. Viktor Tóth for a careful reading of our paper and many fruitful comments. W.-S. Jeong acknowledges a Japan Society for the Promotion of Science (JSPS) fellowship to Japan. We thank Myungshin Im, Bon-Chul Koo, and Michael Rowan-Robinson for helpful suggestions. The UK participation to the AKARI project is supported in part by PPARC/STPC. The Korean participation to AKARI project is supported by the KRF Grant No.R14-2002-01000-0 and BK21 program to SNU.

References

- Finkbeiner, D. P., Davis, M., & Schlegel, D. J. 1999, *ApJ*, 524, 867
 Gautier, T. N., III, Boulanger, F., Péroult, M., & Puget, J. L. 1992, *AJ*, 103, 1313
 Jeong, W.-S., et al. 2005, *MNRAS*, 357, 535
 Jeong, W.-S., Pearson, C. P., Lee, H. M., Pak, S., & Nakagawa, T. 2006, *MNRAS*, 369, 281
 Kawada, M., et al. 2007, *PASJ*, 59, S389
 Kiss, Cs., Klaas, U., & Lemke, D. 2005, *A&A*, 430, 343
 Miville-Deschênes, M.-A., & Lagache, G. 2002, *ApJS*, 157, 302
 Murakami, H. 1998, in *Proc. SPIE 3356, IR Space Telescopes and Instruments*, ed. P. Y. Bely & J. B. Breckinridge (Bellingham, WA: SPIE), 471
 Murakami, H., et al. 2007, *PASJ*, 59, S369

- Nakagawa, T. 2001, in Proc. The Promise of the Herschel Space Observatory, ed. G. L. Pilbratt, J. Cernicharo., A. M. Heras, T. Prusti, & R. Harris, ESA SP-460 (Nordwijk: ESA), 67
- Pearson, C. P., et al. 2004, MNRAS, 347, 1113
- Schlegel, D. J., Finkbeiner, D. P., & Davis, M. 1998, ApJ, 500, 525
- Shibai, H., 2004, Adv. Space Res., 34, 589
- Soifer, B. T, Houck, J. R., & Neugebauer, G. 1987, ARA&A, 25, 187
- Wheelock, S. L., et al. 1994, IRAS Sky Survey Atlas: Explanatory Supplement (Pasadena: JPL 94-11)